Palaeogeography, Palaeoclimatology, Palaeoecology 598 (2022) 111017

Contents lists available at ScienceDirect

Palaeogeography, Palaeoclimatology, Palaeoecology

journal homepage: www.elsevier.com/locate/palaeo

Carbon and oxygen isotope fractionation in the Late Devonian heterocoral *Oligophylloides*: Implications for the skeletogenesis and evolution of the Heterocorallia

Patrycja G. Dworczak [a,b,*], Matthias López Correa [b,c], Michał Jakubowicz [d], Axel Munnecke [b], Michael M. Joachimski [e], Claudio Mazzoli [f], Błażej Berkowski [a]

[a] Institute of Geology, Adam Mickiewicz University, ul. Bogumiła Krygowskiego 12, Poznań 61-680, Poland
[b] Geozentrum Nordbayern, Friedrich-Alexander-Universität Erlangen-Nürnberg, Loewenichstr. 28, Erlangen D-91054, Germany
[c] Consiglio Nazionale delle Ricerche, Istituto di Scienze Marine, via Gobetti 101, Bologna I-40129, Italy
[d] Isotope Research Unit, Adam Mickiewicz University, ul. Bogumiła Krygowskiego 10, Poznań 61-680, Poland
[e] Geozentrum Nordbayern, Friedrich-Alexander-Universität Erlangen-Nürnberg, Schloßgarten 5, Erlangen D-91054, Germany
[f] Department of Geosciences, University of Padova, Via V. Gradenigo, 6, Padova I-35131, Italy

ARTICLE INFO

Editor: Prof. Thomas Algeo

Keywords:
Heterocorallia
Cnidaria
Carbon and oxygen isotopes
Microstructure
Morocco
Poland

ABSTRACT

The order Heterocorallia is an enigmatic, anatomically distinct group of calcifying Palaeozoic corals with unclear affinities to other, either extinct or modern cnidarian lineages. Here, we present results of microstructure and stable isotope studies on exceptionally well-preserved skeletons of two species of the heterocoral *Oligophylloides* from the Famennian (Upper Devonian) of the Anti-Atlas, Morocco and the Holy Cross Mountains, Poland. The investigations provide new information on the skeletogenesis and isotope fractionation effects in Palaeozoic heterocorals. In order to estimate the possible role of diagenetic alteration on the observed carbon and oxygen isotope ratios, we have conducted several preservation tests, including transmitted-light, scanning-electron, fluorescence and cathodoluminescence microscopy, Raman spectroscopy, and trace element analyses. The least- and most-altered skeleton portions identified based on this approach are typified by clearly different isotopic signatures. The least-altered parts of the specimens reveal carbon and oxygen isotope ratios close to those of contemporaneous marine-equilibrated calcites. The moderately-pronounced, positive correlations between the $\delta^{13}C$ and $\delta^{18}O$ values observed for these coralla may reflect relatively minor vital fractionation effects, obscured to some degree by diagenetic overprint. The results suggest that the isotope fractionation mechanisms of the heterocorals differed markedly from the significant kinetic fractionation characteristic of the modern scleractinian corals. Rather, the moderate, if any, extent of non-equilibrium fractionation during skeletogenesis in the Heterocorallia resembled the typical, environmental and metabolic CO_2-dominated fractionation effects shown by most other marine calcifiers. These include the extinct rugose corals, modern hydrocorals and, in particular, modern octocorals, with which the heterocorals show notable architectural and structural similarities.

1. Introduction

Stable isotope research on fossil corals is mostly applied to palaeoenvironmental and palaeoecological reconstructions. The interpretation of the collected data is complicated by defining the primary mineralogy of extinct coral taxa (e.g. Brand and Veizer, 1980; Brand, 1981b). Moreover, the interpretation may be strongly influenced by possible vital effects, unknown past seawater composition, and, most importantly, potential diagenetic alteration (Berkowski and Belka, 2008; Jakubowicz et al., 2015). During interactions between the skeletal carbonate and diagenetic fluids, the stable isotope and trace element records may be shifted towards equilibrium with diagenetic waters as a result of dissolution, recrystallization and precipitation of cements (Veizer et al., 1997). The potential for alteration of the primary signatures depends primarily on the isotopic system studied, the type of diagenetic fluids, their isotopic composition and elemental concentrations, as well as the minerals involved and the cumulative fluid-rock ratio (Banner and Hanson, 1990; Ahm et al., 2018). The alteration

* Corresponding author at: Institute of Geology, Adam Mickiewicz University, ul. Bogumiła Krygowskiego 12, Poznań 61-680, Poland.
E-mail address: patrycja.dworczak@amu.edu.pl (P.G. Dworczak).

https://doi.org/10.1016/j.palaeo.2022.111017
Received 9 November 2021; Received in revised form 19 April 2022; Accepted 24 April 2022
Available online 28 April 2022

may occur during early diagenesis, when the isotope signatures and temperature of the diagenetic fluids are similar to seawater (Veizer et al., 1997; Girard et al., 2017). Consequently, recognizing the primary skeletal mineralogy, the quality of microstructural preservation and physical separation of cements from the pristine coral skeletons remain the key challenges for geochemical studies on Palaeozoic corals (Brand, 1981a, 1983; Popp et al., 1986a; Allison et al., 2007; Coronado et al., 2013; Zapalski, 2014). It is generally accepted that low-magnesium calcite is diagenetically more stable than the other calcium carbonate polymorphs, high-magnesium calcite and, in particular, aragonite (e.g. Allan and Matthews, 1982; Veizer et al., 1997; Auclair et al., 2003; van Geldern et al., 2006; Brand et al., 2019). Unlike the extant, aragonitic scleractinian corals, as well as the Palaeozoic rugose and tabulate corals, which skeletons contained moderate concentrations of Mg ('intermediate Mg calcite', 5–8 mol% $MgCO_3$) (e.g. Brand, 1981a; Sorauf, 1996; Sorauf and Webb, 2003), a primary low-magnesium calcite mineralogy was suggested for the Palaeozoic heterocorals (Fedorowski, 1991; Scrutton, 1997; Chwieduk, 2001; Berkowski et al., 2021). The original mineralogy was determined primarily based on the notably well-preserved microstructure commonly observed in the Heterocorallia – irregular lamellae with sharp outlines, oriented perpendicularly to the corallum growth direction (Chwieduk, 2001). Hence, provided careful material selection and identification of the best-preserved parts of the coralla, the very thick, compact walls of the heterocoral skeletons appear a suitable material for determining their primary stable isotope signatures. This includes also the potential to explore the presence of non-equilibrium isotope fractionation effects, so-called 'vital effects'. The latter, reflecting metabolic, kinetic and/or physiological controls on the calcification processes (e.g., in aragonitic Scleractinia: Rollion-Bard et al., 2010; Oppelt et al., 2017; in calcitic gorgonian octocorals: Hill et al., 2011; Chaabane et al., 2019), have implications for better understanding both the skeletogenesis and the evolutionary relationships among the various groups of skeletonised cnidarians (cf., Jakubowicz et al., 2015).

Here, we provide the first report on the stable carbon and oxygen isotope composition of two species of *Oligophylloides* Różkowska, 1969, the most studied Devonian genus of the heterocorals. The Heterocorallia Schindewolf, 1941 is an extinct order of Palaeozoic corals, relatively poorly represented in the Devonian and Carboniferous fossil record. The first, although questionable, records of heterocorals are known from the early Eifelian (Fernández-Martínez et al., 2003), and the last occurrences were noted in the Serpukhovian (Weyer and Polyakova, 1995), but there are long-time gaps in their occurrence in the Givetian, Frasnian and Tournaisian, while they are relatively common in the late Famennian and Viséan. Nonetheless, complete coralla are extremely rare (Weyer, 2016) due to the fragile architecture of their skeletons, composed of long and thin branches. Hence, in most cases they are found as isolated, broken branches lacking their proximal and distal parts, or as massive basal colony parts (Dworczak et al., 2020).

The origin and affinities of heterocorals are still debatable. To date, three main views on the evolutionary relationships of the Heterocorallia have been presented: (1) that they derived from rugose corals (Fedorowski, 1991; Oliver, 1996); (2) that they evolved from other, non-skeletonised cnidarians (see discussion in: Scrutton, 1997); and, most recently, (3) that they should be included in the Octocorallia, as they display many skeletal homologies to the octocorals, notably to some taxa of the *Keratoisidinae* within the *Isididae* (Berkowski et al., 2021). The main skeletal characters to distinguish the heterocorals from other calcifying cnidarians is the lack of a calyx, epitheca and centrifugal insertion of septal-like structures (e.g. Różkowska, 1969; Fedorowski, 1991; Wrzołek, 1993; Chwieduk, 2001; Berkowski, 2002; Weyer, 2016; Berkowski et al., 2021). For decades, each branch of a heterocoral was regarded as a corallite – the skeleton of a single polyp with its own septal apparatus. Thus, most heterocorals were treated as solitary organisms, only rarely forming weakly integrated colonies. However, a recent study of Berkowski et al. (2021), performed on morphologically perfectly preserved specimens of the Famennian heterocoral *Oligophylloides*, has shown that the branches represent a skeleton of a multipolyp colony, implying that the heterocorals must have been strictly colonial organisms. The stable isotope analyses presented here, performed on four apparently well-preserved specimens of two *Oligophylloides* species and including rigorous preservation tests (transmitted-light, scanning-electron, fluorescence and cathodoluminescence microscopy, Raman spectroscopy and accessory trace element analyses) aimed at distinguishing the primary isotope signatures, provide new constraints on the skeleton secretion mechanisms and evolutionary affinities of the Heterocorallia.

2. Geological setting

Three specimens of *Oligophylloides maroccanus* were collected from the Famennian (Upper Devonian) strata exposed at Jebel Bou Ifarherioun, eastern Anti-Atlas, Morocco (31°7′59.20"N; 4°17′9.84"W). The Jebel Bou Ifarherioun section comprises a Givetian to Famennian carbonate succession formed in the south-western part of the Tafilalt Platform, within a wide shelf marking the passive margin of north-western Gondwana (Fig. 1A, B) (e.g., Wendt, 1985; Wendt and Belka, 1991; Belka et al., 1997; Lubeseder et al., 2010; Wendt, 2021). The specimens were collected from upper Famennian, grey to reddish crinoid wackestones/packstones, which were dated to the middle/late *Palmatolepis gracilis expansa* conodont Zone sensu Ziegler and Sandberg (1984). The limestone contains abundant ammonoids, especially specimens of *Gonioclymenia speciosa*, well-preserved heterocoral fragments, and deep-water solitary rugose corals, as well as reworked and broken remains of invertebrates and vertebrates (Dworczak et al., 2020).

The specimen of *Oligophylloides pachythecus* was collected from the Łagów-Dule section in the Holy Cross Mountains, Poland, where a Famennian succession (*Palmatolepis rhomboidea* to early *Palmatolepis trachytera* conodont zones) is well exposed (Czarnocki, 1989; Dzik, 2006; Wilk et al., 2019). During the Middle Devonian, the southern part of the Holy Cross Mountains constituted a broad, shallow-water carbonate platform located at subtropical latitudes (Fig. 1A, C) (Szulczewski, 1995; Szulczewski et al., 1996). The investigated heterocoral specimen was collected from dark-coloured, bituminous limestones with abundant macrofossils (cephalopods, crinoids, gastropods, fishes, stromatoporoids and trilobites) and microfossils (foraminifera, ostracods and conodonts). The fossils and co-occurring pyrite indicate that the heterocorals inhabited a deep-shelf, dysoxic environment (Chwieduk, 2001). The limestone was dated to the *Palmatolepis marginifera* conodont Zone sensu Ziegler and Sandberg (1984).

3. Material

The investigated material comprises three *O. maroccanus* specimens (UAM He/JBI/10, hereinafter referred to as M1, UAM He/JBI/11; hereinafter referred to as M2, UAM He/JBI/12, hereinafter referred to as M3) from Morocco (Fig. 2A–D) and one *O. pachythecus* specimen (UAM He/HCM/Ro1, hereinafter referred to as PL) from Poland (Fig. 2E). The material represents fragments of heterocoral branches, 4 to 9 mm in diameter (Fig. 2). These specimens have been cut transversally and longitudinally into thin sections and polished slabs. Longitudinal stem sections of the coralla M2, M3 and PL were cut along the central axis, while the longitudinal section of the specimen M1 was slightly off-centre.

3.1. *Oligophylloides maroccanus* Weyer, 2016

3.1.1. Description

Heterocoral formed a fan-shaped corallum. Thick-walled branches can bifurcate and their diameters range from 10 to 20 mm, thinning distally. The central core is 0.4–0.7 mm wide. In the lumen, there are 8–12 parasepta (3 generations), which can continue into the

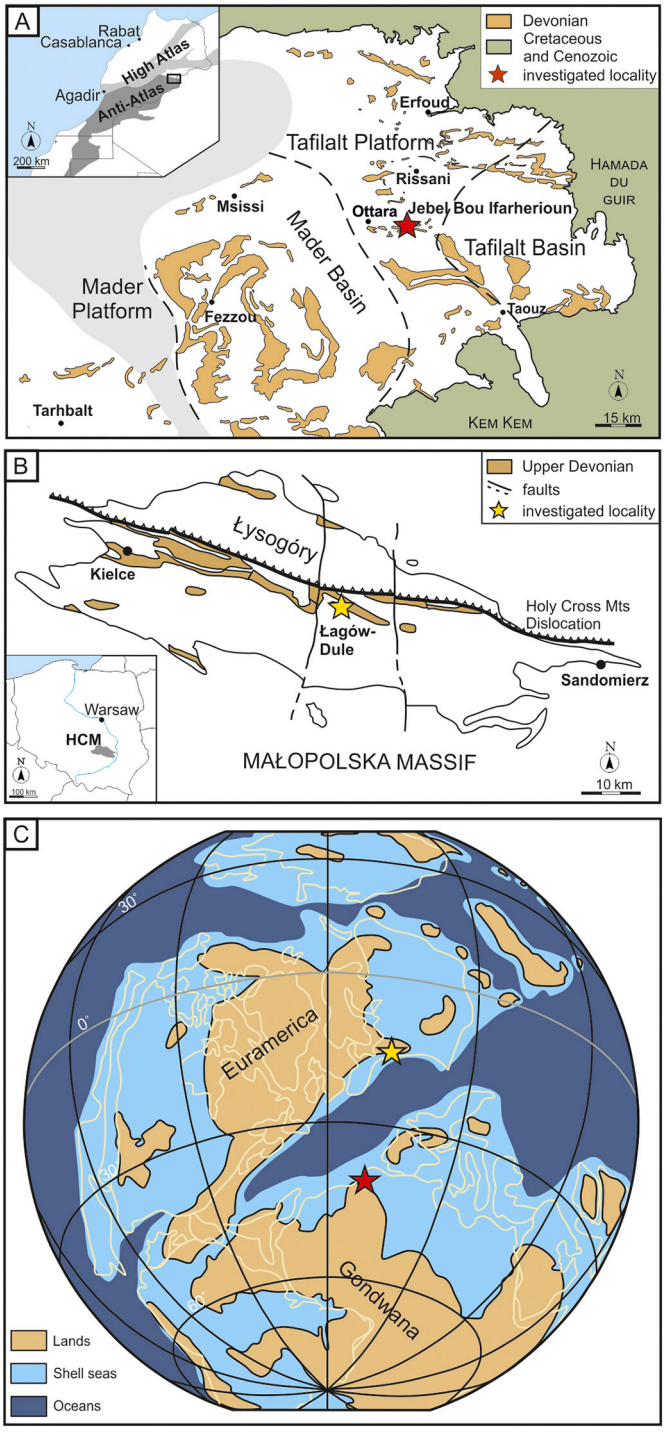

Fig. 1. A. Collection site of the studied upper Famennian coralla of *Oligophylloides maroccanus* (specimens M1, M2 and M3): the Jebel Bou Ifarherioun section (red star), eastern Anti-Atlas, Morocco. The geological map shows the outcrop distribution of the Devonian strata and the main Devonian sedimentary basins of the eastern Anti-Atlas (slightly modified after Jakubowicz et al., 2019, adapted from Dopieralska, 2009); B. Collection site of the studied middle Famennian specimen of *Oligophylloides pachythecus*: the Łagów-Dule section (yellow star), Holy Cross Mountains, Poland (HCM). The distribution map of the Upper Devonian deposits (according to Kowalczewski, 1971); C. The Late Devonian map of Earth (Scotese, 2001), red star – Anti-Atlas, and yellow star – Holy Cross Mountains. (For interpretation of the references to colour in this figure legend, the reader is referred to the web version of this article.)

protoheterotheca. Outer surfaces of the branches are smooth.

3.1.2. Remarks

The investigated stem fragments are cylindrical and oval in transverse section, with the diameter of 9 to 15 mm and the central core of about 0.5 mm width (Fig. 2A–D, 4D–F). Three generations of parasepta are visible (Fig. 3C).

3.2. *Oligophylloides pachythecus* Różkowska, 1969

3.2.1. Description

It is a colonial coral, with a branch diameter between 0.5 and 5 mm. The stem wall varies in thickness; the central core takes up ¼ of the width. Outer wall surfaces are smooth and their microstructure is lamellar. Branches are polygonal or cylindrical in cross section and possess 5 to 16 parasepta (most frequently 10). In places, remnants of parasepta occur as zigzag paths within the protoheterotheca (Berkowski, 2002).

3.2.2. Remarks

The branch fragment studied here is cylindrical in transverse section, with the central core taking up to ¼ of the stem (Fig. 2E). Three generations of parasepta are visible in the lumen; they continue in the protoheterotheca (Fig. 4J–L).

The heterocoral coralla from Morocco were collected during our fieldwork campaign in 2019, whereas the specimen from the Holy Cross Mountains was collected by Prof. Maria Różkowska. All specimens are housed in the collection of the Adam Mickiewicz University in Poznań.

4. Methods

4.1. Thin sections

The preliminary microstructural observations, and the initial preservation evaluation aimed at guiding the subsequent microscopic, trace element and isotopic analyses, were performed based on petrographic thin-sections of 35 μm thickness, prepared at the Adam Mickiewicz University. The heterocoral branches were first photographed and then cut transversally and longitudinally with a diamond blade. Sections of the samples were glued to glass slides in epoxy resin and polished with silicon carbide powder (1000–800 grit). Additionally, the transmitted-light observations in conjunction with the cathodoluminescence and fluorescence microscope analyses guided the selection of the Micromill tracks for the stable carbon and oxygen isotope analyses.

4.2. Cathodoluminescence microscopy

The cathodoluminescence investigations, aimed at visualising the internal structure, growth lines and diagenetically-altered parts of the coralla, were carried out with a Cambridge.

luminoscope system CITL 8200 mk3 (“cold cathode” type), operating under 10–12 kV accelerating voltage and 200–250 μA beam current at the Adam Mickiewicz University.

4.3. Fluorescence microscopy

A LEICA DM 5000 B fluorescence microscope (FL) housed at the Biology Department of the University of Padova, Italy, was used to illustrate the internal architecture, banding, porosity and diagenetic modifications in the studied specimens. The LEICA CTR 5000 light source was applied in conjunction with a GFP filter, and the emitted fluorescence was recorded at various intensities and magnifications with a digital camera (LEICA DFC 425C). Data were processed with the LEICA Application Suite 4.4.0.

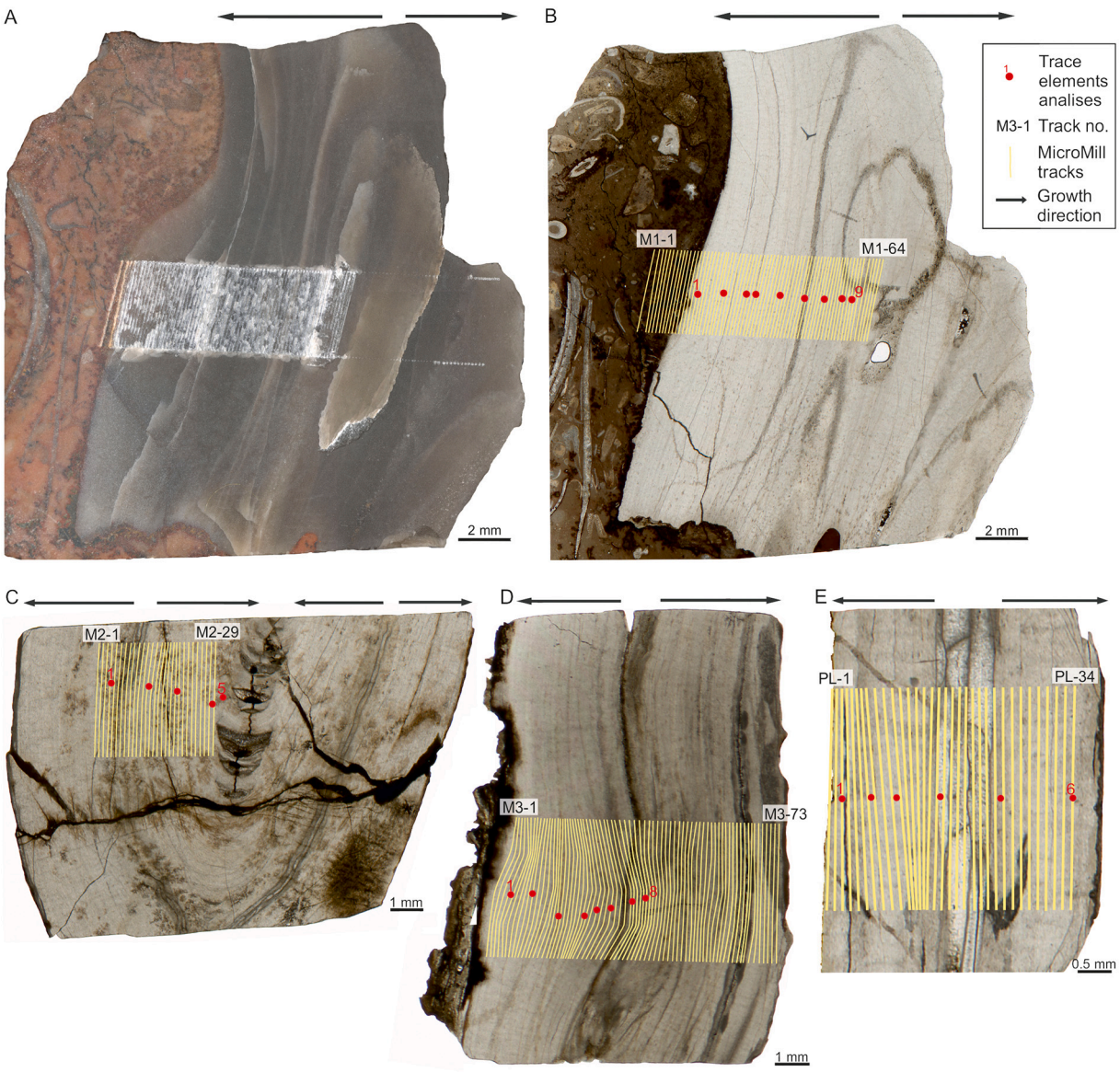

Fig. 2. Polished slabs and thin sections of the studied species of the Famennian heterocoral *Oligophylloides*, with indicated position of the Micromill sampling tracks for stable isotopes and the electron-microprobe spot measurements for trace element analysis. A–B. *O. maroccanus*, Anti-Atlas, Morocco, specimen M1, sequentially polished longitudinal slab and thin section. Note that the longitudinal thin section was cut below the surface of the polished slab; C–D. *O. maroccanus*, Anti-Atlas, Morocco, specimens M2 (C) and M3 (D); E. *Oligophylloides pachythecus*, Holy Cross Mountains, Poland, specimen PL.

4.4. Micro-Raman spectroscopy

Coral mineralogy was explored with a Thermo Scientific micro-Raman Spectroscope at the Chemistry Institute of the University of Padova, equipped with a 532 nm DXR laser. The monochromatic laser light with 532 nm wave-length and a laser power of 3 mW was applied with a 25 μm pinhole and a 50× long-working distance (LWD) objective. The Raman-shift was recorded from 100 to 3500 cm^{-1} with relative intensities measured in counts per second (cps). For spot measurements, the collection exposure time was 30 s and the reported spectra represent averages from four exposures. The acquired spectra were processed with the Omnic software and compared with reference spectra from the RRUFF-database (http://rruff.info/) and in-house standards to identify the skeletal mineralogy. Additionally, characteristic areas with different skeletal elements, like parasepta, theca and diagenetic crystal fillings, were mapped at the 8 × 8 μm spatial resolution (2 × 10 s dwell time).

4.5. Scanning electron microscopy

Cross-sections of all four specimens were cut next to the Micromill transects for stable isotope analyses (see below) and investigated with scanning electron microscopy (SEM) to document the internal architecture and changes from diagenetic processes. Polished sections were etched with 0.1 N HCl for 25 s, rinsed in distilled water, dried at 35 °C and then gold-sputter-coated. The investigations were carried out with a VegaTescan SEM at the Geozentrum Nordbayern of Friedrich-Alexander-Universität Erlangen-Nürnberg, Germany. Secondary electron (SE) and back-scattered electron (BSE) images were taken as mosaic-transects across the entire branch diameter. Accelerating voltage was 20 kV.

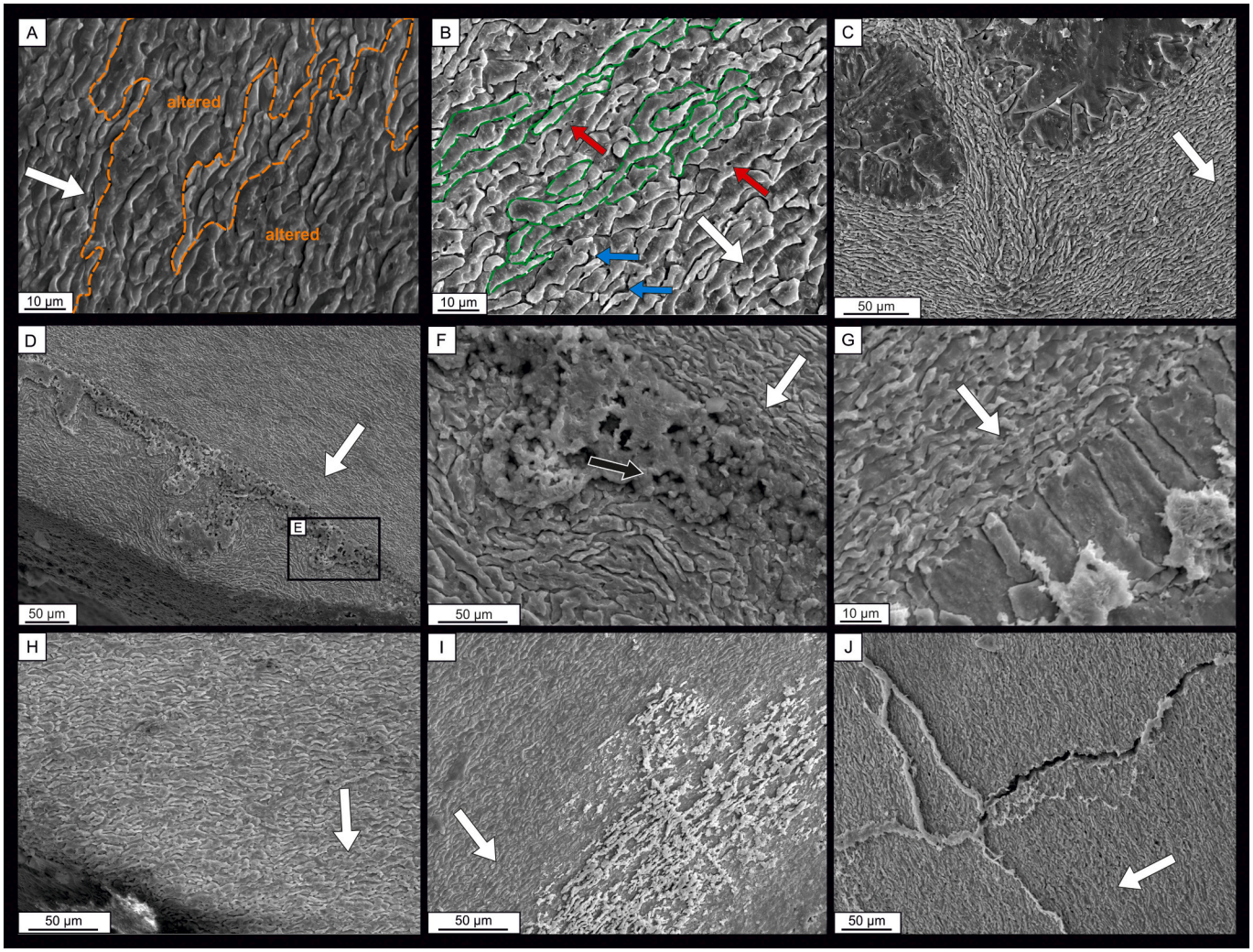

Fig. 3. Scanning Electron Microscope images of polished and etched transverse sections of *Oligophylloides maroccanus*, specimens M1, M2 and M3, Morocco and *Oligophylloides pachythecus*, PL, Poland. A. Specimen M3, altered microstructure, vermiform calcite crystals with molten, very weakly distinguishable boundaries (orange lines); B. Specimens M2, apparently well-preserved skeletal microstructure consisting of calcitic lamella. As an example, a few unaltered crystals (green line), intercrystal porosity (blue) and intracrystal porosity (red) are shown. C. Specimen PL, a paraseptum and the secondarily cement-filled central core. Each single sparry calcite crystal precipitated in crystallographic continuity from a single heterocoral lamella; D. Specimen M1, growth interruption surface and precisely overgrown crystals of protoheterotheca; *E*-F. Close-ups of D; G. Specimen M1, a well-preserved skeleton margin with a sharp boundary between the protoheterotheca and the skeleton-rimming diagenetic sparry cement. Each sparry calcite crystal crystallized from a single heterocoral crystal; H. Specimen M3, the outer part of the skeleton with visibly recrystallized microstructure with fused lamella; I. Specimen M1, recrystallization of calcite crystals and secondary filled empty spaces (likely silica replacement); J. Specimen PL, a secondary crack and adjacent well-preserved microstructure. The white arrows show the growth direction of the calcite lamella, towards the outer margin of the skeleton. (For interpretation of the references to colour in this figure legend, the reader is referred to the web version of this article.)

4.6. Elemental analysis

Based on the cathodoluminescence, scanning electron and fluorescence microscopy, and micro-Raman spectroscopy, the diagenetically least-altered parts of the heterocorals were identified for subsequent, complementary elemental analyses. Graphite-coated polished thin sections were analysed with a Cameca SX-100 electron microprobe at the Inter-Institute Analytical Complex for Minerals and Synthetic Substances, in the Electron Microprobe Laboratory of the University of Warsaw, Poland. The measurements were performed in a WDS (X-ray wavelength dispersive spectroscopy) mode under 15 kV accelerating voltage, 20 nA beam current and 25 µm spot diameter. Five elements (Ca, Mg, Mn, Fe, Sr) were targeted at each sampling spot. The following standards, analytical lines and crystals were used: Ca (Kα, PET), Mg (Kα, TAP) - diopside; Mn (Kα, LPET) - rhodonite; Fe (Kα, LIF) - hematite; and Sr (Lα, TAP) celestine. A ZAF matrix correction (*Z*-atomic number correction, A-absorption correction, F-fluorescence correction) was applied to all analyses. Detection limits for each analysis are given in Table S1.

4.7. Stable isotope analysis

Sampling for the stable isotope measurements was carried out with a Merchantek New Wave Micromill at the Geozentrum Nordbayern of Friedrich-Alexander Universität Erlangen-Nürnberg. The heterocoral specimens were cut into longitudinal sections to enable sampling of ontogenetic transects from the innermost layers to the external margin. The sampling tracks were placed parallel to the growth bands, with an average spacing of 150 µm. The track length was 3.0 mm, with a final milling depth of 150 µm at a width of ~100 µm. Drill-bit rotation was set to 80% at a scan speed of 100 µm/s. The carbon and oxygen isotope ratios were then analysed at the Geozentrum Nordbayern. All carbonate powders were reacted with 100% phosphoric acid at 70 °C using a Gasbench II connected to a Thermo-Fisher Delta V Plus mass

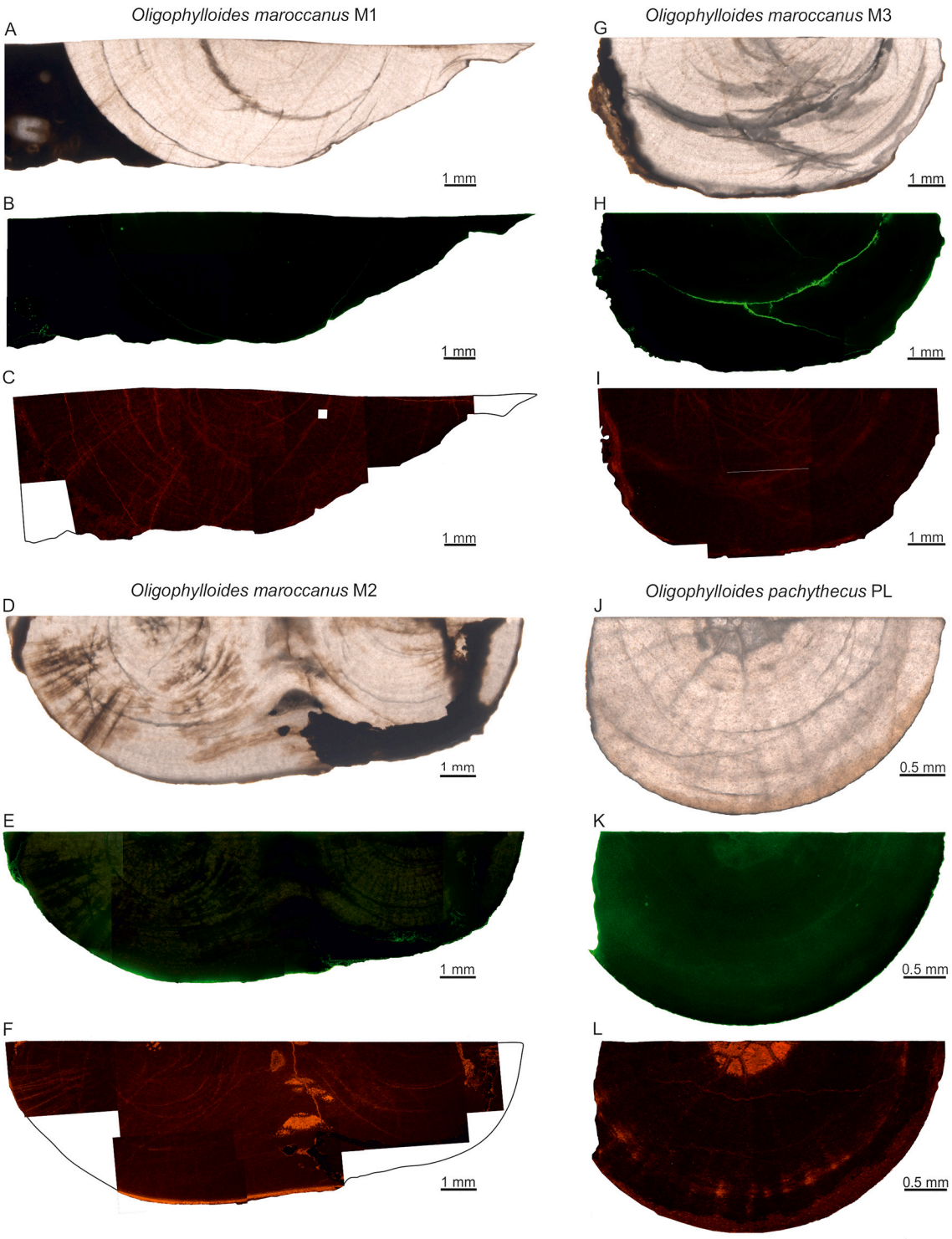

Fig. 4. Transmitted light, fluorescence and cathodoluminescence microscopy images of transverse sections. A–C. *Oligophylloides maroccanus*, Anti-Atlas, Morocco, specimen M1; D–F. *O. maroccanus*, Anti-Atlas, Morocco, specimen M2; G–I. *O. maroccanus*, Anti-Atlas, Morocco, specimen M3; J–L. *O. pachythecus*, Holy Cross Mountains, Poland, specimen PL.

spectrometer. All values are reported in per mil (‰) relative to V-PDB by assigning a $\delta^{13}C$ value of +1.95‰ and a $\delta^{18}O$ value of −2.20‰ to NBS19. In addition to NBS19, IAEA-CO9 was used as a standard for $\delta^{13}C$ with an assigned value of −47.3‰. NBS19 and NBS18 were assigned to $\delta^{18}O$ values of −2.2‰ and − 23.2‰, respectively. External precision and reproducibility were checked by replicate analyses of laboratory standards, and are better than ±0.06‰ (1σ).

5. Results

5.1. Microstructure

The studied heterocoral sections represent, in general, apparently well-preserved primary microstructure, with specific areas showing different levels of diagenetic alteration (Fig. 3A). The SEM observations show that the best visible original microstructural features are typically

found in the central parts of the branches (Fig. 3B–C). The microstructure is formed by irregular lamellae, which are oriented perpendicular to the growth direction of the corallite. The skeletal calcite crystals precisely follow the shape of the heterocoral surface and, if present, of growth interruption surfaces (Fig. 3D, E). Additionally, in the transverse thin sections and SEM images, there are visible continuations of parasepta in the wall (radial structures in protoheterotheca, Figs. 3C; 4J, L). The contact between the open spaces in the central core and the heterotheca is sharp. A similarly sharp contact is visible between the heterotheca and sediment in the specimen M1, where a sparitic rim precipitated around the corallum (Fig. 3G). In both cases, single heterocoral crystals served as nucleation sites for the sparite crystals, which developed during sediment cementation. The crystal sizes are different in both species. Unaltered crystals are max. 4–5 μm in thickness and 18 μm in length for *O. maroccanus*, and max. 2–3 μm in thickness and 20 μm in length for *O. pachythecus*. The smallest crystals are observed in the specimen M2. The walls are very dense and compact, with no major open spaces and intraskeletal porosity (Fig. 3A). The recrystallized microstructure is conspicuous near fissures and outer parts of the branches (Fig. 3F–H) and show vermiform crystals and varying degrees of fusion of adjacent lamella. These parts of the skeleton show also visible porosity. We recognized intracrystal porosity (the porosity present within a crystal; Fig. 3B, red arrows) and intercrystal porosity (empty spaces among calcite crystals; Fig. 3B, blue arrows). However, the SEM investigations show that altered crystals are not always visible in close proximity to the fissures (Fig. 3J). In the specimen M3 (Fig. 3I), partial replacement of the original microstructure with silica(?) is observed.

The cathodoluminescence patterns of individual skeletons are mostly relatively homogeneous, but show differences among the specimens (Fig. 4C, F, I, L). The inner portions of the *O. maroccanus* specimen M2 and the *O. pachythecus* specimen are largely non-luminescent, whereas the *O. maroccanus* specimens M1 and M3 show dull to red luminescence. The outer parts of the *O. maroccanus* specimen M3 and the *O. pachythecus* specimen reveal red luminescence (Fig. 4 C, E, G). Additionally, tiny fissures following the growth lines and perpendicular to some larger fissures show dull to red luminescence. Clear red to orange luminescence occurs in the central cores. In addition, the specimen M2 reveals orange luminescence in the open spaces formed between two branches during development of their heterotheca (Fig. 4F; cf., Weyer, 2016).

All of the studied skeletons display no fluorescence or dull fluorescence (Fig. 4B, E, H, KJ). The specimens M1 and M3 show bright fluorescence in the fissures (Fig. 4B, F). Moreover, the *O. maroccanus* specimen M2 and the *O. pachythecus* specimen show partially bright fluorescence in the outer parts of the branches (Fig. 4D, H). The secondary sparitic cements fill initial spaces between the parasepta in the central cores of the *O. maroccanus* coralla M2 and M3, and the *O. pachythecus* skeleton shows dull fluorescence. The banding and growth lines are weakly visible in the fluorescence images.

The Raman spectra in the skeletons of *O. maroccanus* and *O. pachythecus* consistently reveal a low Mg-calcite mineralogy with four principal peaks of the internal (ν_1; ν_4) and lattice (L; T) modes, centred at 1085.6 cm^{-1} (ν_1), 711.9 cm^{-1} (ν_4), 281.2 cm^{-1} (L), and 154.5 cm^{-1} (T). These four principal peak positions overlap for parasepta, heterotheca and matrix in all samples. The Raman mapping results show that all studied heterocorals have the same distribution pattern of the peaks, and the strongest peaks are typical of the heterotheca.

5.2. Trace elements

The trace element composition of the heterocoral skeletons is given in Table S1. Concentrations of the analysed major (Ca) and minor (Mg, Mn, Fe, Sr) elements show differences among the heterocoral specimens, reflecting their preservation states. For all three samples of *O. maroccanus*, Fe contents are below the detection limits. Increased Fe concentrations (389 and 521 ppm) have been observed only for 2 measurements in *O. pachythecus*, the other samples also falling below the detection limits. Additionally, with a single exception, all of the Mn measurements in *O. pachythecus* are below the detection limit (189 ppm). For the specimen M1, the Mn contents mostly fall between 310 and 511 ppm (with two measurements being below the detection limit: 155 and 170 ppm), for the specimen M2 mostly between 217 and 914 ppm (one measurements below the detection limit: 132 ppm), and for the specimen M3 mostly between 271 and 713 ppm (two measurements below the detection limit: 15 and 155 ppm). The lowest contents of Mn are usually observed in the non-luminescent parts of the skeletons. The highest contents of Mg (3950–6573 ppm) are observed in the non-luminescent parts of *O. pachythecus* from Poland. The specimens M1 and M3 display Mg contents ranging from 3673 to 4469 ppm and 2961 to 5114 ppm, respectively; the lowest Mg concentrations (2099–3160 ppm) typify the *O. maroccanus* specimen M2 (Table S1). The contents of Sr fall between 347 and 541 ppm for the *O. pachythecus* specimen PL, 397 and 1065 ppm for the *O. maroccanus* specimen M1, 178 and 609 for the *O. maroccanus* specimen M2 (with a single measurement below the detection limit of 178 ppm), and 381 and 744 ppm for the *O. maroccanus* specimen M3. Distribution of the measurements in the heterocoral skeleton is shown in Fig. 2 (B–E).

5.3. Stable isotopes

The results of carbon and oxygen isotope analyses are given in Table S2. These data demonstrate some variability in the $\delta^{13}C$ and $\delta^{18}O$ values, not only among the studied heterocoral specimens, but also within different areas of individual branches. In each case, the strongly altered portions of the coralla display $\delta^{13}C$ and/or $\delta^{18}O$ signals distinct from those of the least-altered parts of the skeletons (Figs. 5 and 6).

The $\delta^{13}C$ values range from −1.3 to +2.1‰ for the specimen M1 and from −0.4 to +1.9‰ for the specimen M3, whereas the specimen M2 and *O. pachythecus* show mostly more negative carbon isotope ratios (−1.7 to +0.1‰ and − 2.5 to +0.8‰, respectively). A trend towards lower $\delta^{13}C$ values can be noticed in *O. pachythecus* (−2.5 to +0.7‰) and *O. maroccanus* (M1: −1.3 to +1.9‰; M2: −1.7 to −1.3‰; M3: +0.6 to +1.5‰) at the margins of the branches. Along fissures in the skeletons, $\delta^{13}C$ values vary from +1.6 to +2.1‰ to for M1, from −1.6 to 0.0‰ for M2 and from −0.4 to +1.9‰ for M3. Additionally, three specimens were cut through the central core filled by sparry cements (Fig. 4). The results from the central cores display distinct $\delta^{13}C$ values (see Fig. 5B, D).

All observed $\delta^{18}O$ values are negative and reveal higher variability than the $\delta^{13}C$ signals. The highest $\delta^{18}O$ values occur in the least-altered skeletal parts: −3.9 to −2.5‰ for the *O. maroccanus* specimen M1, −4.8 to −2.6‰ for the *O. maroccanus* specimen M3 and − 5.7 to −4.3‰ for the *O. pachythecus* specimen PL. In the heterocorals from Morocco, the overall $\delta^{18}O$ values range from −10.9 to −2.5‰ for M1, −7.3 to −4.8‰ for M2 and − 6.8 to −2.4‰ for M3. The smallest range of $\delta^{18}O$ values is observed in *O. pachythecus* from Poland (−6.0 to −4.3‰). For the samples collected along the branch margins, the oxygen isotope signals are most negative: −10.9 to −3.4‰ for the specimen M1, from −7.3 to −6.3‰ for the specimen M2, from −6.8 to −3.1‰ for the specimen M3 and from −5.5 to −5.4‰ for *O. pachythecus*. $\delta^{18}O$ values from the fissures range from −5.6 to −2.6‰ for M1, from −6.2 to −5.6‰ for M2 and from −4.6 to −2.8‰ for M3. The samples cut through the branch centre (Fig. 5B–D) show slightly more negative values (see Fig. 5B, C, D and Table S2).

6. Discussion

The stable isotope data collected in the present study, together with the integrated picture provided by the employed multi-proxy preservation tests: transmitted-light, scanning-electron, fluorescence and cathodoluminescence microscopy, Raman spectroscopy and accessory trace element analyses, define two general trends in the isotope composition

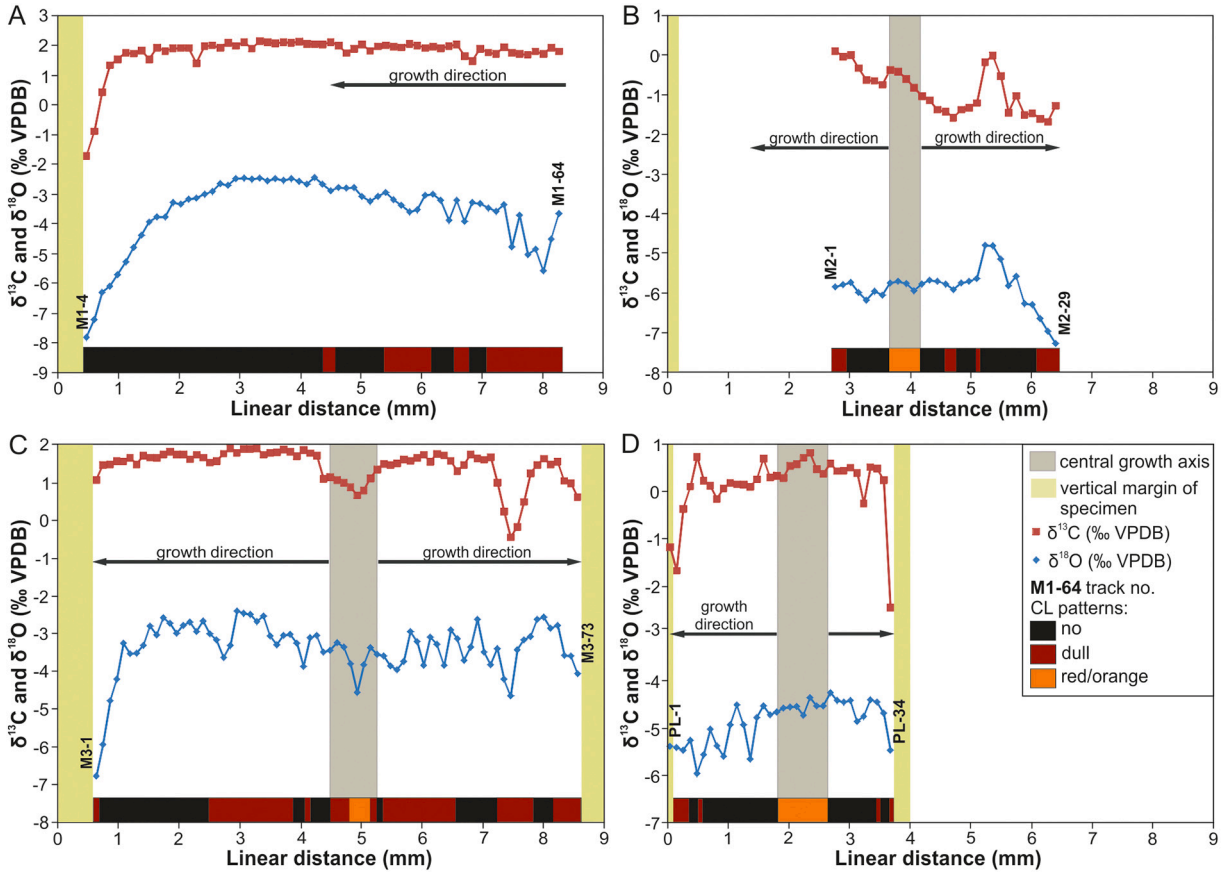

Fig. 5. Results of the stable carbon isotope and oxygen isotope analyses from ontogenetic Micromill transects with marked growth direction (black arrows), external branch margins (light green bars), central growth axis (grey bars), and cathodoluminescence responses. A. *Oligophylloides maroccanus* Anti-Atlas, Morocco, specimen M1; B. *O. maroccanus*, Anti-Atlas, Morocco, specimen M2; C. *O. maroccanus*, Anti-Atlas, Morocco, specimen M3; D. *O. pachythecus*, Holy Cross Mountains, Poland, specimen PL. (For interpretation of the references to colour in this figure legend, the reader is referred to the web version of this article.)

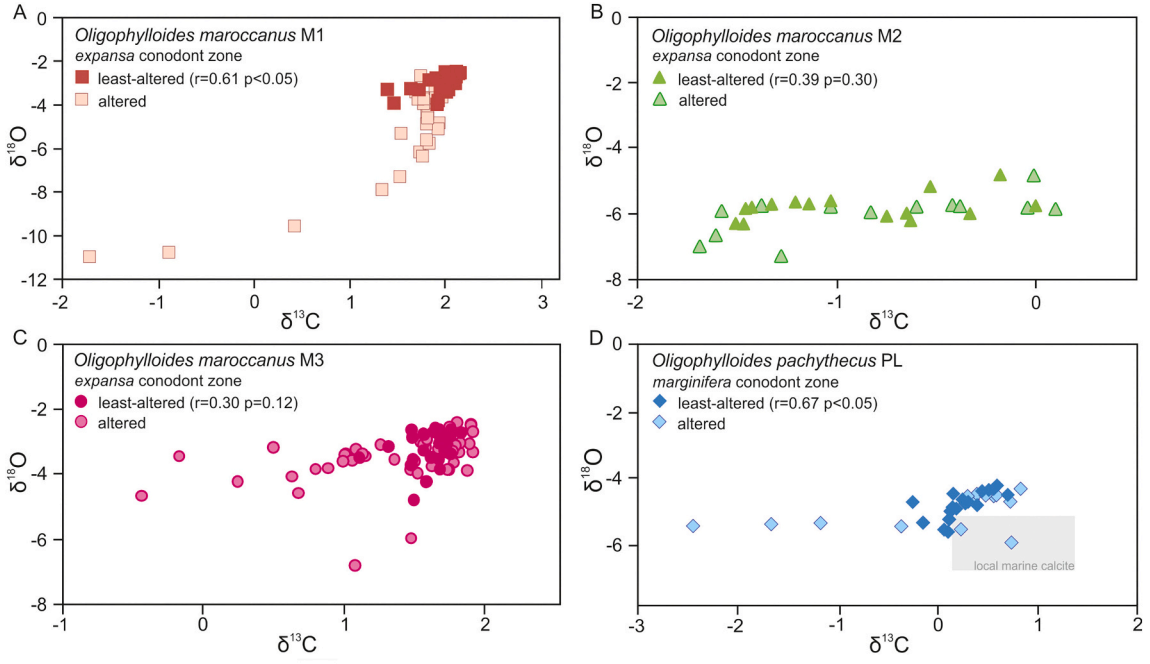

Fig. 6. Stable carbon vs. oxygen isotopes ratios in *Oligophylloides* spp. A. *Oligophylloides maroccanus* Anti-Atlas, Morocco, specimen M1; B. *O. maroccanus*, Anti-Atlas, Morocco, specimen M2; C. *O. maroccanus*, Anti-Atlas, Morocco, specimen M3; D. *O. pachythecus*, Holy Cross Mountains, Poland, specimen PL. The range defined for middle Famennian marine-equilibrated calcites (brachiopod shells) from the Holy Cross Mountains by Hałas et al. (1992) is also shown.

of the studied heterocoral skeletons: (1) the specimens, and the portions of individual specimens, identified as best-preserved based on the series of microscopic investigations are characterised by a relatively low variability of the $\delta^{13}C$ and $\delta^{18}O$ values, apparently falling close to the values of coeval marine-equilibrated calcites; (2) the samples recognized as most altered commonly show carbon and, in particular, oxygen isotope ratios deviating from the background marine signal. Below, we interpret the observed stable isotope values in the context of the preservation of individual specimens, and discuss their implications for understanding the fractionation mechanisms and evolutionary affinities of Palaeozoic heterocorals.

6.1. *Stable isotope composition: The primary vs. diagenetic signatures*

Among the analysed *O. maroccanus* corals from Morocco, two specimens (M1 and M3) reveal a relatively low variability in their $\delta^{18}O$ and, in particular, $\delta^{13}C$ signals. In the skeleton portions recognized as best-preserved based on the combination of the applied diagenetic-screening methods (cf., Berkowski and Belka, 2008; Wisshak et al., 2009; Jakubowicz et al., 2015; Oppelt et al., 2017), the observed variability in the $\delta^{13}C$ and $\delta^{18}O$ values is within 0.5‰ (see Fig. 7). In general, the studied specimens show some of the best examples of microstructure preservation among Palaeozoic corals. This is in line with the results of other studies on the Heterocorallia, commonly documenting relatively well-preserved skeletons, a pattern apparently reflecting their skeletal Mg contents being lower than in other groups of Palaeozoic calcifying anthozoans (e.g., Scrutton, 1997; Sorauf and Webb, 2003; Chaabane et al., 2019; Flöter et al., 2019). The exceptionally preserved corallum portions reveal lamellar microstructure, best visible under SEM, with calcite crystals oriented parallel to the branch margins, following their shape and perpendicular to the growth direction. This type of microstructure preservation attests to a minor degree of material exchange within, rather than between the laminae, and thus typically entails a limited degree of diagenetic elemental exchange (see Jakubowicz et al., 2015 and references therein). Accordingly, the bulk of these well-preserved skeletons show non-luminescence, a feature indicative of no significant input of Mn^{2+} ions from reducing, diagenetic fluids, attesting to the limited elemental exchange experienced by the coralla during the diagenesis (cf., Popp et al., 1986b; Habermann et al.1998; Melim et al., 2002; Brand, 2004). Locally more pronounced cathodoluminescence responses may be attributed to the areas of increased porosity, allowing for fluid percolation and, despite the well-preserved laminae, precipitation of diagenetic calcite within the inter-crystalline spaces (cf., Casella et al., 2016). While precipitation of such cements might have resulted in some shifts of the original stable isotope ratios, the potential of fluid circulation through such small intraskeletal pores to strongly alter the isotope signatures of the primary skeletal material remains likely limited. Accordingly, in the studied specimens the variability of the $\delta^{13}C$ values is consistently very low. On the other hand, areas of significant alternation of the skeletons caused by diagenetic fluids are readily identifiable as changes in the cathodoluminescence responses and the pattern of the microstructure preservation. Such areas most typically occur on to the outer parts of the skeletons and in proximity to cement-filled fissures, and are usually characterised by a distinct depletion in ^{13}C as compared to well-preserved skeletal parts.

Diagenetic alteration and precipitation of inter-crystalline cements can also affect the Mn and Fe contents in carbonate skeletons. Carbonates precipitated from oxygenated seawater typically have low concentrations of Mn and Fe, below 200 ppm and 600 ppm, respectively (Denison et al., 1994; Brand et al., 2003). Indeed, the best-preserved parts of the specimens M1 and M3 are mostly characterised by comparatively low Mn contents (M1: bdl to 511 ppm and M3: bdl to 713 ppm). The relatively high detection limits inherent to the microprobe measurements leave some uncertainty for the lower limit of the observed Mn-concentration variability. Nevertheless, the relatively low Mn concentrations in the microstructurally well-preserved parts of the coralla are supported by their non-luminescence, because activation of luminescence may occur at Mn concentrations as low as 10 ppm (Habermann et al., 1998). In this context, the apparent contradiction between the lack of luminescence and increased Mn contents born by some of the measurements may be explained by the very small scale of the microprobe analyses, which may illustrate local inhomogeneities in the element distribution, insufficient to affect the larger-scale luminescence patterns. The generally low Mn contents are accompanied by increased Mg (M1: 3673 to 4469 ppm; M3: 2961 to 4209 ppm) and Sr (M1: 397 to 1065 ppm; M3: 3381 to 600 ppm) concentrations, which are also typical of well-preserved carbonate materials, as these elements tend to be removed from the carbonate crystal lattice in the course of diagenesis

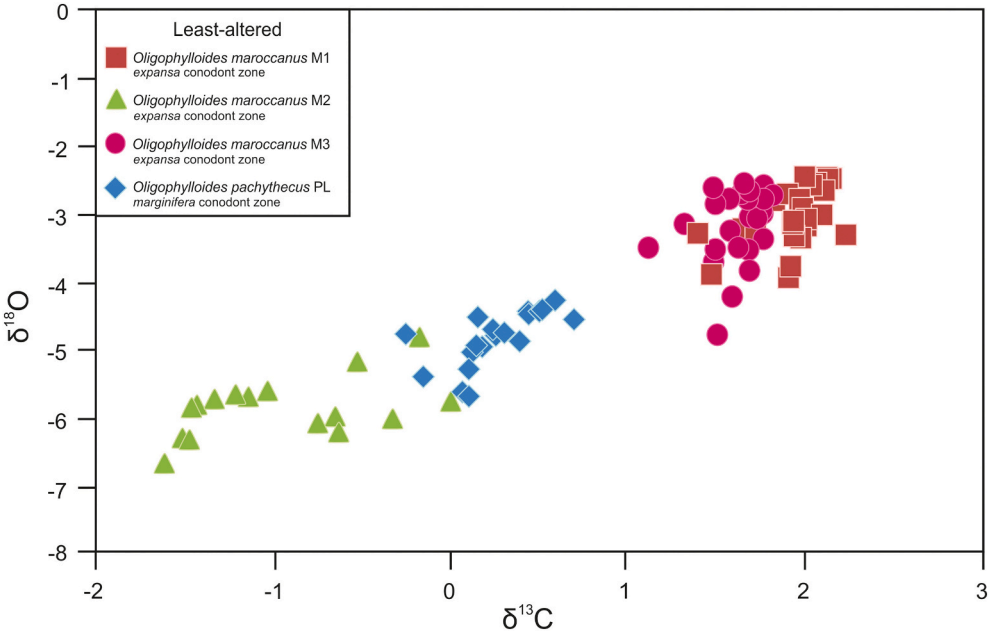

Fig. 7. Comparison of stable carbon vs. oxygen isotope ratios of the least-altered skeleton parts of *Oligophylloides maroccanus* Anti-Atlas, Morocco (specimens M1, M2 and M3), and of *Oligophylloides pachythecus*, Holy Cross Mountains, Poland (specimen PL).

(Tucker and Wright, 1990). Generally, enrichment of the carbonates in Mn and Fe indicates some degree of diagenetic exchange, because, to be incorporated in the carbonate crystals, Fe(III) and Mn(IV) must be anaerobically reduced to Fe(II) and Mn(II), respectively. However, the Mn and Fe incorporation is also dependent on the mineralogy, with the rhombohedral crystal lattice of calcite being notably more favourable for incorporation of Mn^{2+} than orthorhombic aragonite (e.g., Reeder, 1983; Finch and Allison, 2007). Thus, the moderately increased concentration of Mn in the primarily low-Mg calcitic, heterocoral skeletons, while implying some diagenetic effect, does not attest to a strong role of diagenesis in modifying the observed isotope signals. Given the minor Mn contents sufficient to activate luminescence in carbonates, this is especially the case for the carbon isotope signals, which alteration would require very high fluid-rock ratios (Banner and Hanson, 1990; Knauth and Kennedy, 2009; Brand et al., 2011).

A similar pattern in the geochemical signals is observed for the *O. pachythecus* specimen from Poland, for which the least-altered portions of the sampled sections show a relatively narrow range of the $\delta^{13}C$ values (−0.3 to +0.7‰). Compared to the Moroccan specimens M1 and M3, the corresponding variability in the $\delta^{18}O$ values (M1: −3.9 to −2.5‰; M3: −4.8 to −2.5‰) is somewhat larger. More notable differences are the generally higher $\delta^{13}C$ values and, in particular, a ^{18}O-depletion shown by the Polish material, reaching 1.7‰ for the $\delta^{18}O$ values (−5.7 to −4.3‰). Besides the well-defined original, lamellar structure and growth banding, the parts of the coralla interpreted as the best-preserved areas are non-luminescent and have the highest Mg contents among all analysed heterocoral specimens. Therefore, while some diagenetic alteration may possibly account for the increased $\delta^{18}O$ variability, especially for the samples accompanied by no shifts in the $\delta^{13}C$ values, we interpret the generally low $\delta^{18}O$ values observed in the specimen from Poland as its primary feature. The required skeleton precipitation from seawater with different temperature and/or oxygen isotope composition appears consistent with the palaeogeographic positions of the Polish Holy Cross Mountains and the Moroccan Anti-Atlas. During the Late Devonian, the two study areas were located on opposite sides of the Rheic Ocean, with the Anti-Atlas located at ca. 35–40°S, and the Holy Cross Mountains situated much closer to the equator (around 15°S; Scotese, 2001; Golonka, 2020). Accordingly, an analogous pattern, with lower corallite $\delta^{18}O$ values observed in the Holy Cross Mountains than in the Anti-Atlas, was previously documented for well-preserved skeletons of Middle Devonian rugose corals (Jakubowicz et al., 2015).

In contrast, the skeleton portions interpreted as diagenetically altered are generally depleted in ^{13}C and, in particular, ^{18}O. The trend is typically towards lower $\delta^{13}C$ and $\delta^{18}O$ values, a pattern that is common in diagenetic carbonates because of the progressive contribution of ^{13}C-depleted carbon from organic matter remineralisation, and increasing pore-water temperatures (Popp et al., 1986a; Veizer et al., 1997; Buggisch and Joachimski, 2006; Kaiser et al., 2008; Wisshak et al., 2009). Diagenetic resetting of the primary signals apparently applies also to the *O. maroccanus* specimen M2, for which the highest measured $\delta^{13}C$ and $\delta^{18}O$ values are still ~2–3‰ lower than the values observed in the specimens M1 and M3. Since all the studied *O. maroccanus* coralla have been collected from coeval strata of a single, deep-water section, the large differences between their stable isotope signals cannot be attributed to spatial differences in temperature or isotope composition of local seawater. Compared to the remaining Moroccan coralla, the specimen M2 is characterised by much lower Mg contents, attesting to diagenetic alteration associated with the neomorphic Mg removal. In general, the corallum M2 is characterised by skeletal inhomogeneities and cement-filled growth-band delaminations (Figs. 2C, 4D–F), as well as a notably smaller branch thickness, all favouring diagenetic elemental exchange (e.g., Harlou et al., 2016). An increased role of diagenetic alteration appears in this case implied also by the clear asymmetry of the variations in the stable isotope signatures with respect to the growth axis (Fig. 5B).

For the Polish specimen PL, as well as the Moroccan specimens M1 and M3, the diagenetic effects are most pronounced in the outermost parts of the skeletons, which, throughout diagenesis, were subjected to the highest degree of interactions with diagenetic fluids. This effect may have also been emphasised by addition of early-diagenetic cements, precipitating both in the intraskeletal spaces and as overgrowths on the corallum surface. In both cases, the cements are commonly syntaxial and can be difficult to identify without using advanced methods, such as Electron Backscatter Diffraction (EBSD) and Laser Ablation, which enable distinguishing biogenic and diagenetic carbonates in nano- and microscale (e.g., Cusack et al., 2008; Balthasar et al., 2021). When found within the inner parts of the branches, in turn, the diagenetically-altered areas are most commonly associated with skeletal inhomogeneities or, most notably, fissures, and thus also subjected to increased circulation of diagenetic solutions. Most commonly, the altered parts can be reliably identified already based on their visibly altered microstructure, as well as their pronounced luminescence responses. This generally supports the usefulness of this method as a simple, cost- and time-effective means of preliminarily evaluation of the preservation state of carbonate materials. Nevertheless, the apparently altered values recorded in places in the essentially non-luminescent part of the specimens M1 and M3 underline also the limitations of this technique as a standalone preservation test in diagenetic screening, and the requirement of using a combination of several methods in order to identify the least-altered parts of the skeleton and ideally primary isotope signals therein. Likewise, examples of both non-luminescence in clearly altered skeletons, as well as luminescence in primary, well-preserved corals have previously been documented (Popp et al., 1986a; Stolarski et al., 2007; Gothmann et al., 2015; Jakubowicz et al., 2015).

6.2. Isotope fractionation in the Heterocorallia

The limited isotope variability observed in the least-altered parts of the studied coralla is in general accord with the deep-water habitats typically suggested for the Heterocorallia, and specifically implied for the studied *O. maroccanus* assemblage by the hemipelagic character of its host succession (Wendt and Belka, 1991; Dworczak et al., 2020). Such environments entail a lack of significant seasonal variability during skeleton growth. In this context, some variations observed in the apparently well-preserved skeleton portions may reflect changes in the growth rate, and associated degree of kinetic vital effects (cf., Heikoop et al., 2000; Marali et al., 2013; Chaabane et al., 2016). Nevertheless, constraining the precise extent of the potential isotope fractionation effects in Palaeozoic corals is generally difficult. The relatively crude precision inherent to the available calcite-based Palaeozoic seawater $\delta^{13}C$ and $\delta^{18}O$ reconstructions enables only approximate comparison with the background, abiotic signatures. For most intervals, the reconstructed marine-calcite signals span a range of a few ‰ (cf., e.g., van Geldern et al., 2006; Veizer and Prokoph, 2015), which hampers recognition of moderate fractionation effects, typical of most calcifying marine animals (cf., Wefer and Berger, 1991; McConnaughey et al., 1997). This group includes also the modern non-scleractinian corals: calcitic octocorals and aragonitic hydrocorals, for which the offset from the equilibrium $\delta^{13}C$ and $\delta^{18}O$ signatures typically ranges from ~0 to +3‰ (Chaabane et al., 2016; Wisshak et al., 2009). For the middle to late Famennian, the reported marine-calcite values fall within the broad ranges of ca. 0 to +3‰ for $\delta^{13}C$ and −1 to −7‰ for $\delta^{18}O$; compared to the other parts of the Devonian, the dataset remains, nevertheless, relatively limited and restricted to low-latitude areas (e.g., Veizer et al., 1999; Brand, 2004; Joachimski et al., 2004; for compilations see Prokoph et al., 2008 and Grossman and Joachimski, 2020). More precise comparisons can be performed for Palaeozoic materials on a case-by-case basis using local archives, preferably well-preserved brachiopods. For the Polish Holy Cross Mountains, the recorded heterocoral stable isotope values fall generally within the range of marine signatures defined previously for middle Famennian brachiopods ($\delta^{13}C = 0$ to 2‰; $\delta^{18}O = -5$ to −6‰; Hałas et al., 1992; Fig. 6D). For the Moroccan Anti-

Atlas, data on the stable isotope composition of strictly coeval marine-equilibrated calcites are, however, lacking, and the scarce upper Famennian brachiopods that we collected from this area were too small to enable reliable isotope measurements. Additionally, the stable isotope measurements on the Famennian rhynchonelloid brachiopod *Dziaduszyckia* from Morocco (Baliński and Biernat, 2003) were not considered, because these brachiopods inhabited hydrocarbon-seep environments (Peckmann et al., 2007).

A clue to identifying minor degrees of isotope fractionation can be provided by analysing covariance patterns within the stable isotope datasets, because in most calcifiers the vital effects are characterised by a positive correlation between the $\delta^{13}C$ and $\delta^{18}O$ values (e.g., Hill et al., 2011; Marali et al., 2013). When only the least-altered portions of the skeletons are analysed, moderate positive correlations can indeed be observed for two of the studied coralla (specimens M1: $r = 0.61$ and PL: $r = 0.67$, both $p < 0.05$; Figs. 6A, D, 7). This may suggest some disequilibrium stable isotope fractionation in *Oligophylloides*. On the other hand, however, even relatively minor admixture of diagenetic intercrystalline cements may also potentially result in development of $\delta^{13}C - \delta^{18}O$ covariance in fossil corals otherwise showing no fractionation effects (cf., Berkowski and Belka, 2008; Jakubowicz et al., 2015). The question of whether the calcitic heterocoral skeletons originally displayed no appreciable fractionation or limited effects similar to those known from the modern octocorals and hydrocorals cannot be, therefore, answered beyond doubt. It is, nevertheless, clear from the collected dataset that the studied species of *Oligophylloides* did not show fractionation effects comparable to those observed in the modern azooxanthellate Scleractinia, in which pronounced kinetic and/or physiological fractionation results in significant ^{13}C- and ^{18}O-depletion (to −5‰ for $\delta^{18}O$ values, and −10‰ for $\delta^{13}C$ values; McConnaughey et al., 1997; Adkins et al., 2003; Marali et al., 2013; Oppelt et al., 2017).

Similarly to the recent study on middle Palaeozoic rugose corals (Jakubowicz et al., 2015), the present contribution adds to the growing evidence that the extreme level of non-equilibrium fractionation observed in the aragonitic azooxanthellate scleractinians (e.g. Adkins et al., 2003; Marali et al., 2013; Oppelt et al., 2017) are an exception, rather than a rule among the modern and fossil calcifying cnidarians. Stable isotope incorporation during skeletogenesis in most marine calcifiers is apparently dominated by environmental and metabolic CO_2, rather than by kinetic effects (cf., McConnaughey et al., 1997). Accordingly, a minor kinetic fractionation is observed in modern calcitic octocorals (Hill et al., 2011; Kimball et al., 2014; Chaabane et al., 2016) and aragonitic hydrocorals (Weber and Woodhead, 1972; Black and Andrus, 2012; Wisshak et al., 2009). Likewise, the comparatively low isotopic variability recorded in Palaeozoic, calcitic rugosans (Berkowski and Belka, 2008; Jakubowicz et al., 2015) and heterocorals (this study) contrasts with the modern bathyal scleractinians, lending further support to the emerging consensus that carbonate skeletons developed independently in the various groups of the skeletonised Cnidaria. In this respect, the results of the present approach place also additional constraints on the evolutionary affinities of the Heterocorallia, and in particular on their recent interpretation as members of the Octocorallia (Berkowski et al., 2021), a group that split from other cnidarians as early as the Ediacaran and most likely became skeletonised during middle Palaeozoic time (Quattrini et al., 2020; McFadden et al., 2021).

7. Conclusions

- We provide the first report on the stable carbon and oxygen isotope composition of Palaeozoic heterocorals. The analyses have been performed on skeletons of two species of the Upper Devonian (Famennian) genus *Oligophylloides*, collected from two localities in the eastern Anti-Atlas (Morocco) and Holy Cross Mountains (Poland).
- The studied heterocorals are generally characterised by exceptionally well-preserved skeletal material, including the fine microstructure detail. Application of multi-proxy, microscopic and trace element diagenetic-screening tests enabled coherent identification of the best-preserved portions of the coralla, suitable for extraction of the original stable isotope signals.
- The least-altered parts of the skeletons consistently show a limited variability of the $\delta^{13}C$ and $\delta^{18}O$ values, in line with a low environmental variability of the heterocoral habitats, reflecting their general preference for deep-water settings. These values fall essentially within the ranges reported for calcites precipitated in equilibrium with contemporaneous seawater, although the published Late Devonian marine-calcite data do not allow for conclusive identification of potential minor non-equilibrium fractionation effects in the heterocorals.
- The skeleton portions recognized as diagenetically altered ones commonly show distinct stable isotope ratios, highlighting the need of careful material selection in isotope studies even for groups characterised by high preservation potential of the original skeletal features, such as the calcitic heterocorals.
- The isotope fractionation effects in the heterocorals were clearly close to the moderate-level fractionation typical of the modern Hydrocorallia and Octocorallia, as well as the extinct Rugosa. The stable isotope incorporation in the heterocoral skeletons must have, therefore, been controlled primarily by the isotope composition of the environmental and, to a lesser degree, respiratory CO_2, rather than by strong kinetic and/or physiological effects comparable to those of the azooxanthellate scleractinians.
- These results contribute to the discussion on evolutionary relationships between the heterocorals and other calcareous cnidarians, including, most importantly, its recently suggested close affinity to the extant octocorals.

Declaration of Competing Interest

On behalf of my co-authors and myself I am declared that no conflict of interests exist.

Acknowledgements

This research was funded the by National Science Center of Poland, Project No. 2017/25/N/ST10/00445 (to PD) and 2019/33/B/ST10/00059 (to BB). The analyses and stay at the University in Erlangen-Nürnberg were funded by the Polish National Agency for Academic Exchange (Iwanowska Programme). We are particularly grateful to Prof. Zdzislaw Belka (Adam Mickiewicz University), who led the field expeditions to Morocco. At the University of Erlangen-Nürnberg, Daniele Lutz kindly performed the stable isotope measurements, Birgit Leipner-Mata assisted with laboratory work, and Emilia Jarochowska provided constructive discussions. Sara Schiavon (University of Padova) facilitated work at the fluorescence microscopes at the Biology Institute. This is CNR-ISMAR Bologna scientific contribution n. 2026. We are greatly indebted to the representatives of the Ministère de l'Energie, des Mines, de l'Eau et de l'Environnement (Morocco), Ahmed Benlakhdim, Khalid El Hmidi and Aissam El Khlifi, for the work permit and logistic advice. The manuscript benefited from helpful comments of two anonymous reviewers and the journal editor, Lucia Angiolini, which are gratefully acknowledged.

Appendix A. Supplementary data

Supplementary data to this article can be found online at https://doi.org/10.1016/j.palaeo.2022.111017.

References

Adkins, J.F., Boyle, E.A., Curry, W.B., Lutringer, A., 2003. Stable isotopes in deep-sea corals and a new mechanism for "vital effects". Geochim. Cosmochim. Acta 67, 1129–1143.

Ahm, A.S.C., Bjerrum, C.J., Blättler, C.L., Swart, P.K., Higgins, J.A., 2018. Quantifying early marine diagenesis in shallow-water carbonate sediments. Geochim. Cosmochim. Acta 236, 140–159.

Allan, J.R., Matthews, R.K., 1982. Isotope signatures associated with early diagenetic meteoric diagenesis. Sedimentology 29, 797–817.

Allison, N., Finch, A.A., Webster, J.M., Clague, D.A., 2007. Palaeoenvironmental records from fossil corals: the effects of submarine diagenesis on temperature and climate estimates. Geochim. Cosmochim. Acta 71, 4693–4703.

Auclair, A.C., Joachimski, M.M., Lécuyer, C., 2003. Deciphering kinetic, metabolic and environmental controls on stable isotope fractionations between seawater and the shell of *Terebratalia transversa* (Brachiopoda). Chem. Geol. 202, 59–78.

Baliński, A., Biernat, G., 2003. New observations on rhynchonelloid brachiopod *Dzieduszyckia* from the Famennian of Morocco. Acta Palaeontol. Pol. 48 (3), 463–474.

Balthasar, U., Kershaw, S., Da Silva, A.C., Seuss, B., Cusack, M., Eichenseer, K., Chung, P., 2021. Palaeozoic stromatoporoids and chaetetids analysed using electron backscatter diffraction (EBSD); implications for original mineralogy and microstructure. Facies 67, 1–18.

Banner, J.L., Hanson, G.N., 1990. Calculation of simultaneous isotopic and trace element variations during water-rock interaction with applications to carbonate diagenesis. Geochim. Cosmochim. Acta 54, 3123–3137.

Belka, Z., Kaufmann, B., Bultynck, P., 1997. Conodont based quantitative biostratigraphy for the Eifelian of the eastern Anti-Atlas, Morocco. Geol. Soc. Am. Bull. 109, 643–651.

Berkowski, B., 2002. Famennian Rugosa and Heterocorallia from southern Poland. Palaeontol. Pol. 61, 3–88.

Berkowski, B., Belka, Z., 2008. Seasonal growth bands in Famennian rugose coral *Scruttonia kunthi* and their environmental significance. Palaeogeogr. Palaeoclimatol. Palaeoecol. 265, 87–92.

Berkowski, B., Zapalski, M.K., Jarochowska, E., Alderslade, P., 2021. Early development and coloniality in *Oligophylloides* from the Devonian of Morocco – are Heterocorallia Palaeozoic octocorals? PLoS One 16 (9), e0257523. https://doi.org/10.1371/journal.pone.0257523.

Black, H., Andrus, C.F.T., 2012. Taphonomy and diagenesis on the deep-sea hydrocoral *Stylaster erubescens* fossils from the Charleston Bump. Univ. Alabama McNair J. 12, 19–40.

Brand, U., 1981a. Mineralogy and chemistry of the lower Pennsylvanian Kendrick fauna, eastern Kentucky. 1. Trace elements. Chem. Geol. 32, 1–16.

Brand, U., 1981b. Mineralogy and chemistry of the lower Pennsylvanian Kendrick fauna, eastern Kentucky. 2. Stable isotopes. Chem. Geol. 32, 17–28.

Brand, U., 1983. Mineralogy and chemistry of the lower Pennsylvanian Kendrick fauna, eastern Kentucky. 3. Diagenetic and palaeoenvironmental analysis. Chem. Geol. 40, 167–181.

Brand, U., 2004. Carbon, oxygen and strontium isotopes in Palaeozoic carbonate components: an evaluation of original seawater-chemistry proxies. Chem. Geol. 204, 23–44.

Brand, U., Veizer, J., 1980. Chemical diagenesis of a multicomponent carbonate system – 1: Trace elements. J. Sediment. Petrol. 50, 1219–1236.

Brand, U., Logan, A., Hiller, N., Richardson, J., 2003. Geochemistry of modern brachiopods: applications and implications for oceanography and paleoceanography. Chem. Geol. 198, 305–334.

Brand, U., Logan, A., Bitner, M.A., Griesshaber, E., Azmy, K., Buhl, D., 2011. What is the ideal proxy of Palaeozoic seawater chemistry? Mem. Assoc. Aust. Palaeontol. 41, 9–24.

Brand, U., Bitner, M.A., Logan, A., Azmy, K., Crippa, G., Agiolini, L., Colin, P., Griesshaber, E., Harper, E.M., Ruggiero, E.T., Häussermann, V., 2019. Brachiopod-based oxygen-isotope thermometer: update and review. Rev. Italian. Palaeontol. Stratigrafia 125, 775–787.

Buggisch, W., Joachimski, M.M., 2006. Carbon isotope stratigraphy of the Devonian of Central and Southern Europe. Palaeogeogr. Palaeoclimatol. Palaeoecol. 240, 68–88.

Casella, L.A., Griesshaber, E., Neuser, R., Stevens, K., Ritter, A.C., Mutterlose, J., Brand, U., Immenhauser, A., Schmahl, W.W., 2016. Microstructural changes reflect the degree of diagenetic alteration in biogenic carbonates. In: EGU General Assembly Conference Abstracts pp. EPSC2016-14893.

Chaabane, S., López Correa, M., Montagna, P., Kallel, N., Taviani, M., Linares, C., Ziveri, P., 2016. Exploring the oxygen and carbon isotopic composition of the Mediterranean red coral (*Corallium rubrum*) for seawater temperature reconstruction. Mar. Chem. 186, 11–23. https://doi.org/10.1016/j.marchem.2016.07.001.

Chaabane, S., López Correa, M., Ziveri, P., Trotter, J., Kallel, N., Douville, E., Montagna, P., 2019. Elemental systematics of the calcitic skeleton of *Corallium rubrum* and implications for the Mg/ca temperature proxy. Chem. Geol. 524, 237–258.

Chwieduk, E., 2001. The biology of the Famennian heterocoral *Oligophylloides pachythecus*. Palaeontology 44, 1189–1226.

Coronado, I., Pérez-Huerta, A., Rodríguez, S., 2013. Primary biogenic skeletal structures in Multithecopora (Tabulata, Pennsylvanian). Palaeogeogr. Palaeoclimatol. Palaeoecol. 386, 286–299.

Cusack, M., England, J., Dalbeck, P., Tudhope, A.W., Fallick, A.E., Allison, N., 2008. Electron backscatter diffraction (EBSD) as a tool for detection of coral diagenesis. Coral Reefs 27, 905–911.

Czarnocki, J., 1989. Klimenie Gór Świętokrzyskich. Pr. Państw. Inst. Geol. 127, 1–91.

Denison, R.E., Koepnick, R.B., Fletcher, A., Howell, M.W., Callaway, W.S., 1994. Criteria for the retention of original seawater 87Sr/86Sr in ancient shelf limestones. Chem. Geol. 112, 131–143.

Dopieralska, J., 2009. Reconstructing seawater circulation on the Moroccan shelf of Gondwana during the late Devonian: evidence from Nd isotope composition of conodonts. Geochem. Geophys. Geosyst. 10, 1–13.

Dworczak, P.G., Berkowski, B., Jakubowicz, M., 2020. Epizoans immured in the heterocoral *Oligophylloides maroccanus* Weyer, 2017: a unique record from the Famennian (Upper Devonian of Morocco). Lethaia 53 (4), 452–461. https://doi.org/10.1111/let.12369.

Dzik, J., 2006. The Famennian "Golden Age" of conodonts and ammonoids in the polish part of the Variscan Sea. Palaeontol. Pol. 63, 1–360.

Fedorowski, J., 1991. Dividocorallia, a new subclass of Palaeozoic Anthozoa. Bull. l'Inst. Royal Sci. Nat. Belgique 61, 21–105.

Fernández-Martínez, E.M., Tourneur, F., López Alcántara, A., 2003. A new Middle Devonian heterocoral from Spain. Acta Palaeontol. Pol. 48, 531–546.

Finch, A.A., Allison, N., 2007. Coordination of Sr and Mg in calcite and aragonite. Mineral. Mag. 71, 539–552.

Flöter, S., Fietzke, J., Gutjahr, M., Farmer, J., Hönisch, B., Nehrke, G., Eisenhauer, A., 2019. The influence of skeletal micro-structures on potential proxy records in a bamboo coral. Geochim. Cosmochim. Acta 248, 43–60.

Girard, C., Cornée, J.-J., Charruault, A.-L., Corradini, C., Weyer, D., Bartzsch, K., Joachimski, M.M., Feist, R., 2017. Conodont biostratigraphy and palaeoenvironmental trends during the Famennian (late Devonian) in the Thuringian Buschteich section (Germany). Newsl. Stratigr. 50, 71–89.

Golonka, J., 2020. Late Devonian Palaeogeography in the framework of global plate tectonics. Glob. Planet. Chang. 186, 103–129.

Gothmann, A.M., Stolarski, J., Adkins, J.F., Schöne, B., Dennis, K.J., Schrag, D.P., Bender, M.L., 2015. Fossil corals as an archive of secular variations in seawater chemistry since the Mesozoic. Geochim. Cosmochim. Acta 160, 188–208.

Grossman, E.L., Joachimski, M.M., 2020. Chapter 10 - Oxygen Isotope Stratigraphy. In: Gradstein, F.M., Ogg, J.G., Schmitz, M.D., Ogg, G.M. (Eds.), Geologic Time Scale. Elsevier, pp. 279–307.

Habermann, D., Neuser, R.D., Richter, D.K., 1998. Low limit of Mn^{2+}-activated cathodoluminescence of calcite: state of the art. Sediment. Geol. 116, 13–24.

Hałas, S., Balinski, A., Gruszczynski, M., Hoffman, A., Malkowski, K., Narkiewicz, M., 1992. Stable isotope record at the Frasnian/Famennian boundary in southern Poland. N. Jb. Geol. Paläont. 3, 129–138.

Harlou, R., Ullmann, C.V., Korte, C., Lauridsen, B.W., Schovsbo, N.H., Surlyk, F., Thibaulta, N., Stemmerik, L., 2016. Geochemistry of Campanian–Maastrichtian brachiopods from the Rørdal-1 core (Denmark): Differential responses to environmental change and diagenesis. Chem. Geol. 442, 35–46.

Heikoop, J.M., Dunn, J.J., Risk, M.J., Schwarcz, H.P., McConnaughey, T.A., Sandeman, I. M., 2000. Separation of kinetic and metabolic isotope effects in carbon-13 records preserved in reef coral skeletons. Geochim. Cosmochim. Acta 64, 975–987.

Hill, T.M., Spero, H.J., Guilderson, T., Lavigne, M., Clague, D., MacAlello, S., Jang, N., 2011. Temperature and vital effect controls on bamboo coral (Isididae) isotope geochemistry: a test of the "lines method". Geochem. Geophys. Geosyst. 12, 1–14. https://doi.org/10.1029/2010GC003443.

Jakubowicz, M., Berkowski, B., López Correa, M., Jarochowska, E., Joachimski, M.M., Belka, Z., 2015. Stable isotope signatures of Middle Palaeozoic ahermatypic rugose corals - deciphering vital effects, alteration patterns, and palaeoecological implications. PLoS One 10 (9). https://doi.org/10.1371/journal.pone.0136289.

Jakubowicz, M., Król, J., Zapalski, M.K., Wrzołek, T., Wolniewicz, P., Berkowski, B., 2019. At the southern limits of the Devonian reef zone: Palaeoecology of the Aferdou el Mrakib reef (Givetian, eastern Anti-Atlas, Morocco). Geol. J. 54, 10–38.

Joachimski, M.M., van Geldern, R., Breisig, S., Buggisch, W., Day, J., 2004. Oxygen isotope evolution of biogenic calcite and apatite during the Middle and late Devonian. Int. J. Earth Sci. Geol. Rundschau 93, 542–553.

Kaiser, S.I., Steuber, T., Becker, R.T., 2008. Environmental change during the Late Famennian and Early Tournaisian (Late Devonian–Early Carboniferous): implications from stable isotopes and conodont biofacies in southern Europe. Geol. J. 43, 241–260.

Kimball, J.B., Dunbar, R.B., Guilderson, T.P., 2014. Oxygen and carbon isotope fractionation in calcitic deep-sea corals: implications for palaeotemperature reconstruction. Chem. Geol. 381, 223–233. https://doi.org/10.1016/j.chemgeo.2014.05.008.

Knauth, L.P., Kennedy, M.J., 2009. The late Precambrian greening of the Earth. Nature 460, 728–732.

Kowalczewski, Z., 1971. Main geological problems in the Holy Cross Mountains. Geol. Quart. 15, 263–283.

Lubeseder, S., Rath, J., Rücklin, M., Messbacher, R., 2010. Controls on Devonian hemi-pelagic limestone deposition analyzed on cephalopod ridge to slope sections, Eastern Anti-Atlas, Morocco. Facies 56, 295–315. https://doi.org/10.1007/s10347-009-0205-5.

Marali, S., Wisshak, M., López Correa, M., Freiwald, A., 2013. Skeletal microstructure and stable isotope signature of three bathyal solitary cold-water corals from the Azores. Palaeogeogr. Palaeoclimatol. Palaeoecol. 373, 25–38. https://doi.org/10.1016/j.palaeo.2012.06.017.

McConnaughey, T.A., Burdett, J., Whelan, J.F., Paull, C.K., 1997. Carbon isotopes in biological carbonates: Respiration and photosynthesis. Geochim. Cosmochim. Acta 61, 611–622.

McFadden, C.S., Quattrini, A.M., Brugler, M.R., Cowman, P.F., Dueñas, L.F., Kitahara, M. V., Paz-García, D.A., Reimer, J.D., Rodríguez, E., 2021. Phylogenomics, origin, and

diversification of Anthozoans (Phylum Cnidaria). Syst. Biol. 70, 635–647. https://doi.org/10.1093/sysbio/syaa103.
Melim, L.A., Westphal, H., Swart, P.K., Eberli, G.P., Munnecke, A., 2002. Questioning carbonate diagenetic paradigms: evidence from the Neogene of the Bahamas. Mar. Geol. 185, 27–53.
Oliver, W.A., 1996. Origins and relationships of Palaeozoic coral groups and the origin of the Scleractinia. Palaeontol. Soc. Papers 1, 107–134.
Oppelt, A., López Correa, M., Rocha, C., 2017. Biogeochemical analysis of the calcification patterns of cold-water corals *Madrepora oculata* and *Lophelia pertusa* along contact surfaces with calcified tubes of the symbiotic polychaete *Eunice norvegica*: Evaluation of a 'mucus' calcification hypothesis. Deep-Sea Res. I 127, 90–104. https://doi.org/10.1016/j.dsr.2017.08.006.
Peckmann, J., Cambell, K.A., Walliser, O.H., Reitner, J., 2007. A Late Devonian hydrocarbon-seep deposit dominated by dimerelloid brachiopods, Morocco. Palaios 22 (2), 112–114. https://doi.org/10.2110/palo.2005.p05-115r.
Popp, B.N., Anderson, T.F., Sandberg, P.A., 1986a. Brachiopods as indicators of original isotopic compositions in some Palaeozoic limestones. Geol. Soc. Am. Bull. 97, 1262–1269.
Popp, B.N., Anderson, T.F., Sandberg, P.A., 1986b. Textural, elemental, and isotopic variations among constituents in Middle Devonian limestones, North America. J. Sediment. Petrol. 56 (5), 715–727.
Prokoph, A., Shields, G.A., Veizer, J., 2008. Compilation and time-series analysis of a marine carbonate $\delta^{18}O$, $\delta^{13}C$, $^{87}Sr/^{86}Sr$ and $\delta^{34}S$ database through Earth history. Earth Sci. Rev. 87, 113–133.
Quattrini, A.M., Rodríguez, E., Faircloth, B.C., Cowman, P.F., Brugler, M.R., Farfan, G.A., McFadden, C.S., 2020. Palaeoclimate Ocean conditions shaped the evolution of corals and their skeletons through deep time. Nat. Ecol. Evol. 4, 1531–1538.
Reeder, R.J., 1983. Crystal chemistry of the rhombohedral carbonates. In: Reeder, R.J. (Ed.), Carbonates: Mineralogy and Chemistry. Mineralogical Society of America, Reviews in Mineralogy, vol. 44, pp. 1–47.
Rollion-Bard, C., Blamart, D., Cuif, J.P., Dauphin, Y., 2010. *In situ* measurements of oxygen isotopic composition in deep-sea coral, *Lophelia pertusa*: Re-examination of the current geochemical models of biomineralization. Geochim. Cosmochim. Acta 74 (4), 1338–1349. https://doi.org/10.1016/j.gca.2009.11.011.
Różkowska, M., 1969. Famennian Tetracoralloid and Heterocoralloid fauna from the Holy Cross Mountains (Poland). Acta Palaeontol. Pol. 16, 1–187.
Scotese, C.R., 2001. Atlas of Earth History. PALEOMAP 870 Project. Arlington, Texas.
Scrutton, C.T., 1997. The Palaeozoic corals, I: origins and relationships. Proc. Yorks. Geol. Soc. 51, 177–208.
Sorauf, J.E., 1996. Geochemical signature of incremental growth: Rugose corals from the Middle Devonian Traverse Group, Michigan. Palaios 11, 64–70.
Sorauf, J.E., Webb, G.E., 2003. The origin and significance of zigzag microstructure in late Palaeozoic *Lophophyllidium* (Anthozoa, Rugosa). J. Palaeontol. 77, 16–30.
Stolarski, J., Meibom, A., Przenioslo, R., Mazur, M., 2007. A cretaceous scleractinian coral with a calcitic skeleton. Science 318 (5847), 92–94.
Szulczewski, M., 1995. Depositional evolution of the Holy Cross Mts. (Poland) in the Devonian and Carboniferous – a review. Geol. Quart. 39, 471–488.
Szulczewski, M., Belka, Z., Skompski, S., 1996. The drowning of a carbonate platform: an example from the Devonian-Carboniferous of the southwestern Holy Cross Mountains, Poland. Sediment. Geol. 106, 21–49.
Tucker, M.E., Wright, V.P., 1990. Carbonate Sedimentology. Blackwell, Oxford, p. 482. https://doi.org/10.1002/9781444314175.
van Geldern, R., Joachimski, M.M., Day, J., Jansen, U., Alvarez, F., Yolkin, E.A., Ma, X.P., 2006. Carbon, oxygen and strontium isotope records of Devonian brachiopod shell calcite. Palaeogeogr. Palaeoclimatol. Palaeoecol. 240, 47–67.
Veizer, J., Prokoph, A., 2015. Temperatures and oxygen isotopic composition of Phanerozoic oceans. Earth Sci. Rev. 146, 92–104.
Veizer, J., Bruckschen, P., Pawellek, F., Diener, A., Polaha, O.G., Carden, G.A.F., Jasper, T., Korte, C., Strauss, H., Azmy, K., Ala, D., 1997. Oxygen isotope evolution of Phanerozoic seawater. Palaeogeogr. Palaeoclimatol. Palaeoecol. 132, 159–172.
Veizer, J., Ala, D., Azmy, K., Bruckschen, P., Buhl, D., Bruhn, F., 1999. $^{87}Sr/^{86}Sr$, $\delta^{13}C$ and $\delta^{18}O$ evolution of Phanerozoic seawater. Chem. Geol. 161, 59–88.
Weber, J.N., Woodhead, P.M., 1972. Stable isotope ratio variations in non-scleractinian coelenterate carbonates as a function of temperature. Mar. Biol. 15, 293–297.
Wefer, G., Berger, W.H., 1991. Isotope palaeontology: growth and composition of extant calcareous species. Mar. Geol. 100, 207–248.
Wendt, J., 1985. Disintegration of the continental margin of northwestern Gondwana: late Devonian of the eastern Anti-Atlas (Morocco). Geology 13, 815–818.
Wendt, J., 2021. Middle and late Devonian palaeogeography of the eastern Anti-Atlas (Morocco). Int. J. Earth Sci. 110, 1531–1544.
Wendt, J., Belka, Z., 1991. Age and depositional environment of Upper Devonian (early Frasnian to early Famennian) black shales and limestones (Kellwasser Facies) in the Eastern Anti-Atlas, Morocco. Facies 25, 51–90.
Weyer, D., 2016. Solitary and/or colonial growth in the Palaeozoic superorder Heterocorallia Schindewolf, 1914 (Eifelian-Serpukhovian). Freib. Forsch. 23, 59–101.
Weyer, D., Polyakova, V.E., 1995. Heterocorallia aus dem Oberen Serpukhovian des Donez Beckens (Unterkarbon, Arnsbergian; Ukraine). Abhandlungen und Berichte für Naturkunde 18, 143–159.
Wilk, O., Woroncowa-Marcinowska, T., Szrek, P., Ginter, M., 2019. Dule section revisited – vertebrate assemblage reveals new information on late Devonian marine ecosystems. Ichthyolith Issues Special Publication 14, 78–79.
Wisshak, M., López Correa, M., Zibrowius, H., Jakobsen, J., Freiwald, A., 2009. Skeletal reorganisation affects geochemical signals, exemplified in the stylasterid hydrocoral *Errina dabneyi* (Azores Archipelago). Mar. Ecol. Prog. Ser. 397, 197–208. https://doi.org/10.3354/meps08165.
Wrzołek, T., 1993. Reconstruction of the distal cone in the Devonian heterocoral *Oligophylloides*. Courier Forschungsintitut Senckenberg 164, 179–183.
Zapalski, M.K., 2014. Evidence of photosymbiosis in Palaeozoic tabulate corals. Proc. R. Soc. B Biol. Sci. 281 (1775), 20132663.
Ziegler, W., Sandberg, C., 1984. *Palmatolepis* based revision of late Devonian conodont zonation. Geol. Soc. Am. Spec. Pap. 196, 179–194.